

1 **Updated analyses of temperature and precipitation extreme indices since the beginning**
2 **of the twentieth century: The HadEX2 dataset**

3
4 MG Donat¹, LV Alexander^{1,2}, H Yang^{1,2}, I Durre³, R Vose³, RJH Dunn⁴, KM Willett⁴, E
5 Aguilar⁵, M. Brunet^{5,21}, J Caesar⁴, B Hewitson⁶, C Jack⁶, AMG Klein Tank⁷, AC Kruger⁸, J
6 Marengo⁹, TC Peterson³, M Renom¹⁰, C Oria Rojas¹¹, M Rusticucci¹², J Salinger¹³, A
7 Sanhouri Elrayah¹⁴, SS Sekele⁸, AK Srivastava¹⁵, B Trewin¹⁶, C Villarroel¹⁷, LA Vincent¹⁸, P
8 Zhai¹⁹, X Zhang¹⁸, S Kitching^{2,20}

9
10 ¹ Climate Change Research Centre, University of New South Wales, Sydney, Australia

11 ² ARC Centre of Excellence for Climate System Science, University of New South Wales,
12 Sydney, Australia

13 ³ NOAA's National Climatic Data Center, Asheville, NC, USA

14 ⁴ Hadley Centre, Met Office, Exeter, UK

15 ⁵ Centre for Climate Change, Dep. Geography, Universitat Rovira i Virgili, Tarragona, Spain

16 ⁶ Climate System Analysis Group, University of Cape Town, Cape Town, South Africa

17 ⁷ Royal Netherlands Meteorological Institute (KNMI), De Bilt, Netherlands

18 ⁸ Climate Service, South African Weather Service, Pretoria, South Africa

19 ⁹ Earth System Science Centre (CCST), National Institute for Space Research (INPE), São
20 Paulo, Brazil

21 ¹⁰ Unidad de Ciencias de la Atmósfera, Universidad de la Republica, Montevideo, Uruguay

22 ¹¹ SENAMHI, Lima, Peru

23 ¹²Departamento de Ciencias de la Atmósfera y los Océanos, Universidad de Buenos Aires,

24 Buenos Aires, Argentina

25 ¹³ Woods Institute for the Environment, Stanford University, Stanford, CA, USA

26 ¹⁴ Sudan Meteorological Authority (SMA), Khartoum, Sudan

27 ¹⁵ India Meteorological Department, Pune-411005, India

28 ¹⁶ Bureau of Meteorology, Melbourne, Victoria, Australia

29 ¹⁷ Oficina de Estudios, Direccion Meteorologica de Chile, Chile

30 ¹⁸ Climate Research Division, Environment Canada, Toronto, Canada

31 ¹⁹ State Key Laboratory of Severe Weather, Chinese Academy of Meteorological Sciences,

32 Beijing, 100081

33 ²⁰ Newcastle University, Newcastle upon Tyne, UK

34 ²¹ Climatic Research Unit, School of Environmental Sciences, University of East Anglia,

35 Norwich, UK

36 (For submission to *J. Geophysical Research, Atmospheres*)

37

38

39

30th July, 2012

40

41

42

43

44 Address for correspondence

45

46 Markus G. Donat

47 Climate Change Research Centre

48 University of New South Wales

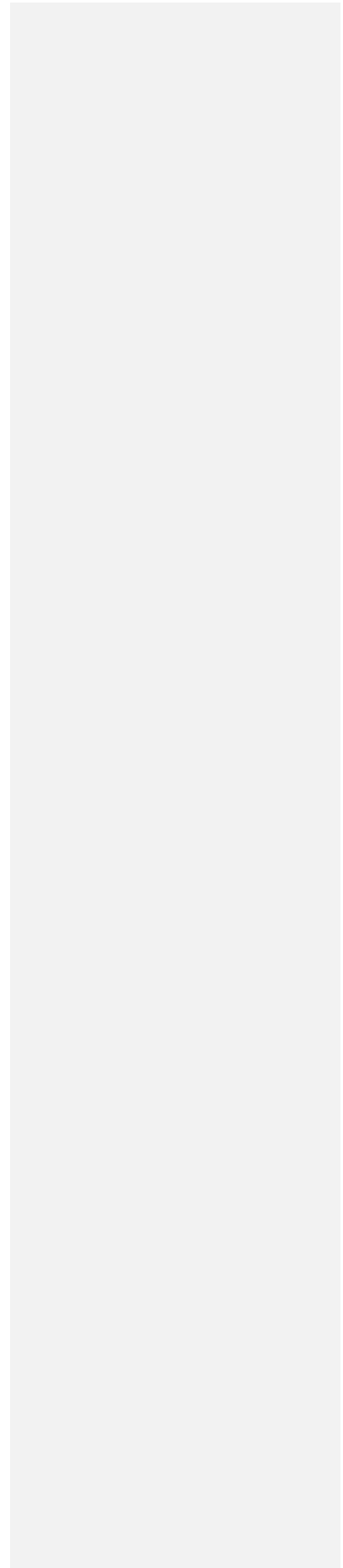
49 Sydney, 2052

50 Australia

51 Ph. +61 2 93858954

52

53 e-mail: m.donat@unsw.edu.au



55 **Abstract**

56 In this study we present the collation and analysis of the gridded land-based dataset of indices
57 of temperature and precipitation extremes: HadEX2. Indices were calculated based on station
58 data using a consistent approach recommended by the WMO Expert Team on Climate
59 Change Detection and Indices, resulting in the production of 17 temperature and 12
60 precipitation indices derived from daily maximum and minimum temperature and
61 precipitation observations. High quality in situ observations from over 6000 temperature and
62 11000 precipitation meteorological stations across the globe were obtained to calculate the
63 indices over the period of record available for each station. Monthly and annual indices were
64 then interpolated onto a 3.75° x 2.5° longitude-latitude grid over the period 1901–2010.
65 Linear trends in the gridded fields were computed and tested for statistical significance.
66 Overall there was very good agreement with the previous HadEX dataset during the
67 overlapping data period. Results showed widespread significant changes in temperature
68 extremes consistent with warming, especially for those indices derived from daily minimum
69 temperature over the whole 110 years of record but with stronger trends in more recent
70 decades. Seasonal results showed significant warming in all seasons but more so in the colder
71 months. Precipitation indices also showed widespread and significant trends, but the changes
72 were much more spatially heterogeneous compared with temperature changes. However,
73 results indicated more areas with significant increasing trends in extreme precipitation
74 amounts, intensity and frequency than areas with decreasing trends.

75

76 1. Introduction

77

78 The research into climate extremes has progressed enormously over the last few decades
79 [Nicholls and Alexander, 2007; Zwiers *et al.*, 2012]. This has been largely due to international
80 coordinated efforts to collate, quality control and analyze variables and events that represent
81 the more extreme aspects of climate. One such effort has been led by the ETCCDI¹
82 (<http://www.clivar.org/organization/etccdi>) who have facilitated the calculation of climate
83 extremes indices based on daily temperature and precipitation data. This has been made
84 possible through the provision of free standardized software for data analysis and quality
85 control, and through the organization of regional workshops to fill in data gaps in data sparse
86 regions [Peterson and Manton, 2008]. Unfortunately, availability of daily observational high-
87 quality data is limited for many regions of the globe. This has several reasons and is partly
88 due to indeed gaps of suitable data, but also many countries have strict restrictions about
89 sharing their data. However, often the national weather services are more happy to share
90 derived annual and monthly indices – which helps to gain information about climate extremes
91 from regions where daily data are not available to the scientific community. Thus, the
92 development of the ETCCDI climate indices has enabled regional and global (both station
93 and gridded) datasets to be developed [Zhang *et al.*, 2011] in a comparable way. One such
94 global gridded dataset, HadEX, was developed by Alexander *et al.*, 2006 (henceforth A2006).
95 HadEX contains the 27 indices recommended by the ETCCDI (see Zhang *et al.*, 2011 and
96 http://cccma.seos.uvic.ca/ETCCDI/list_27_indices.shtml) on a 3.75° x 2.5° longitude-latitude
97 grid from 1951 to 2003. In general one index value was computed per gridbox per year,

¹ Joint World Meteorological Organization (WMO) Commission for Climatology (CCI)/World Climate Research Programme (WCRP) project on Climate Variability and Predictability (CLIVAR)/Joint WMO-Intergovernmental Oceanographic Commission of the United Nations Educational, Scientific and Cultural Organization (UNESCO) Technical Commission for Oceanography and Marine Meteorology (JCOMM) Expert Team on Climate Change Detection and Indices.

98 although for some of the indices (e.g. hottest day/night, wettest day) seasonal values were
99 also made available.

100

101 HadEX currently represents the most comprehensive global gridded dataset of temperature
102 and precipitation extremes based on daily in situ data available. It has been used in many
103 model evaluations (e.g. *Sillmann and Roekner, 2008; Alexander and Arblaster; 2009*
104 *Rusticucci et al., 2010; Sillmann et al., 2012*) and detection and attribution studies (e.g. *Min*
105 *et al., 2011; Morak et al., 2011*), in addition to climate variability and trend studies (e.g.
106 A2006). Nonetheless, it covers a relatively short period (53 years) and contains numerous
107 data gaps both in space and time, and this is particularly the case for the precipitation indices.

108

109 The purpose of the current study is to update HadEX to develop the HadEX2 dataset, and to
110 document and assess this new dataset. This new version of the dataset contains many more
111 input station data than the earlier version of the dataset and covers a much longer period,
112 1901 to 2010. In the next sections we describe the data and indices used as input to HadEX2,
113 the gridding method used to develop grids of the different extremes indices and the analysis
114 of this dataset over global land areas.

115

116 **2. Data and Indices**

117

118 All of the climate indices are calculated from daily observations of precipitation, maximum
119 temperature, and minimum temperature. The indices calculated for HadEX2 are shown in
120 Table 1. These mostly represent the indices recommended by the ETCCDI (see
121 <http://ccma.seos.uvic.ca/ETCCDI/indices.shtml>), although one of the recommended 27
122 indices is user-defined (Rnnmm: annual count of precipitation above a user-chosen threshold)

123 and is therefore excluded and three additional indices are included: Extreme Temperature
124 Range (ETR), contribution from very wet days (R95pTOT), and contribution from extremely
125 wet days (R99pTOT) as these were also included in HadEX due to their potential to have
126 significant societal impacts. A total of 29 indices are therefore calculated. The original station
127 network used in HadEX contained 2223 temperature and 5948 precipitation stations (see Fig.
128 1 of A2006). The total number of stations available for HadEX2 is generally about twice that
129 available for HadEX (see Table 1), including improved spatial coverage of stations in
130 southern Africa, South America, south-east Asia and Australasia. The (monthly) index values
131 were only calculated if less than 3 daily observations were missing in a month, and
132 accordingly less than 15 daily observations per year for the annual indices. If more daily
133 observations were missing, the climate index was set to missing value for this specific month
134 or year. The annual index values are also set to missing if one of the months was assigned a
135 missing value.

136
137 The spatial coverage of stations varies among indices, and there are many more stations
138 containing precipitation than temperature data. It is generally necessary to have a larger
139 number of representative precipitation stations since the spatial variability of precipitation
140 extremes is much higher than for temperature extremes [Kiktev *et al.*, 2003; A2006]. Fig. 1a
141 and 1d show the spatial coverage of stations for an example temperature (TXx) and
142 precipitation (Rx1day) index. The color coding in the maps in Fig. 1 indicates the data
143 source. The largest number of stations was obtained from international data initiatives
144 including:

- 145 1. The European Climate Assessment and Dataset (ECA&D; *Klok and Klein Tank,*
146 2009), containing approximately 6600 stations from 62 countries across Europe and
147 North Africa

- 148 2. The Southeast Asian Climate Assessment and Dataset (SACAD) – as ECA&D but
149 currently containing more than 1000 stations from 11 countries across south-east Asia
- 150 3. The Latin American Climate Assessment and Dataset (LACAD) – as ECA&D but
151 currently containing about 300 stations from 7 countries across Latin America
- 152 4. The Global Historical Climatology Network-Daily (GHCN-Daily; *Menne et al.*,
153 2012). Comprising approximately 27,000 stations globally with daily maximum and
154 minimum temperature and over 80,000 stations with daily precipitation amounts,
155 GHCN-Daily is used in this study only for a subset of its stations in the USA.
156 Although subjected to a comprehensive set of quality assurance procedures (*Durre et*
157 *al.*, 2010), GHCN-Daily data are not adjusted for artificial discontinuities such as
158 those associated with changes in observation time, instrumentation, and station
159 location. To circumvent this, the subset chosen for the USA followed the analysis by
160 *Peterson et al.*, [2008] who only selected National Weather Service Cooperative and
161 First-Order weather observing sites with reasonably long records Data were used
162 only from station time series that were determined (e.g., by the statistical analysis
163 described in Menne and Williams, 2005) to be free of significant discontinuities after
164 1950 caused by changes in station location, changes in time of observation, etc.

165

166 Other stations used in this study have been supplied by the authors either through their
167 personal research or from the National Meteorological Service in that country. For all
168 regions, at least one of the authors had access to the daily data from which the indices were
169 calculated. Therefore reference could always be made to the original data should quality
170 issues arise during the analysis (see Table 2). Additional stations were obtained through
171 ETCCDI regional workshops; although in a small number of cases the raw data were not
172 available and only the derived indices were provided.

173

174 While the level of quality control varies from country to country, in most cases the data have
175 been carefully assessed for quality and homogeneity by researchers in the country of origin.
176 For example, Canada supplied homogenized daily temperatures up to 2010 for 338 stations
177 [Vincent et al., 2012] and a high-quality adjusted precipitation data set for 464 stations
178 [Mekis and Vincent, 2011]. Australian temperature records were updated from those used in
179 HadEX, adjusting for inhomogeneities at the daily timescale by taking account of the
180 magnitude of discontinuities for different parts of the distribution, increasing the number of
181 stations available to 112 and extending the record back in time to 1910 (Trewin, 2012).
182 Indian data have only been used from India Meteorological Department (IMD) observatory
183 stations where exposure conditions have remained the same and meteorological instruments
184 are maintained as per WMO guidelines. In Argentina and Uruguay stations with known
185 inhomogeneities or long periods without data were excluded from the index calculation. In
186 the case of the ETCCDI workshop data, extensive post-processing and analysis was
187 performed [e.g. Aguilar et al., 2009; Caesar et al., 2011; Vincent et al., 2011] to ensure data
188 quality and homogeneity. Note therefore that because of the updates to high quality station
189 availability for many regions, HadEX2 provides not just an extension of stations used in
190 HadEX but rather represents the latest acquisition of high quality station data around the
191 globe.

192

193 Table 2 indicates the sources of all the data used in this study and relevant references where
194 applicable. However since the spatial coverage deteriorated in some cases between HadEX
195 and HadEX2, particularly for Africa and parts of South and Central America, the station
196 coverage was supplemented using existing stations from HadEX where there were no stations
197 in HadEX2 within a 200km radius of a HadEX station. This provided about an additional 200

198 stations for temperature indices and 800 stations for precipitation indices. While the addition
199 of HadEX stations offers some improvement in coverage, data included in HadEX2 are still
200 sparse at the beginning and end of the record in addition to some stations only having short
201 records. Particularly in the most recent years since 2006 there is a decrease in the number of
202 available observational data, which also leads to a strong decline in spatial coverage of
203 HadEX2 during the last five years (Fig. 2) Data for both temperature and precipitation prior to
204 1950 are mostly confined to Eurasia, North America, Southern South America, Australasia
205 and India (precipitation only).

206
207 To ensure consistency in the calculation of indices between regions, the
208 RCLimDex/FClimDex software packages were used (see *Zhang et al.*, 2011 and
209 <http://cccma.seos.uvic.ca/ETCCDI/software.shtml>). Percentiles required for some of the
210 temperature indices (Table 1) were calculated for the climatological base period 1961-1990
211 using a bootstrapping method proposed by *Zhang et al.*, [2005]. The bootstrapping approach
212 is intended to eliminate possible inhomogeneities at the boundaries of the climatological base
213 period due to sampling error. The percentiles are only calculated if at least 75 per cent of
214 daily temperatures during the base period are non-missing values. In addition, problems with
215 data precision have arisen in some countries such as rounding to whole degree in recording,
216 and this can also affect trend estimates for some indices [*Zhang et al.*, 2009]. This has been
217 accounted for by adding a small random number to improve the granularity of data and thus
218 making the estimation of threshold more accurate [*Zhang et al.*, 2009; *Zhang et al.*, 2011].

219
220 Note, however, that the data for ECA&D, SACAD and LACAD were processed slightly
221 differently. These groups calculate many more indices than recommended by ETCCDI but
222 the output from these datasets is processed in such a way as to be comparable with the output

Comentario [MD1]: I think it was 85% in our Fclimdex settings, but Relimdex uses 75%. Not sure about ECA, SACAD, etc.?

223 from RClimDex/FClimDex for the ETCCDI indices. One exception is the calculation of very
224 wet days (R95p) and extremely wet days (R99p). While these indices commonly refer to the
225 precipitation amount above the respective percentile value, ECA&D, SACAD and LACAD
226 instead counted the number of days when the percentile is exceeded. For this analysis, we
227 therefore recalculated their data for these two indices from the calculated values of R95pTOT
228 and PRCPTOT (i.e., $R95pTOT * PRCPTOT / 100$), so that they matched the index definition
229 proposed by the ETCCDI, and in turn providing a consistent analysis approach for all
230 regions.

231

232 **3. Gridding method**

233

234 Our gridding method closely follows that of HadEX (see Appendix A of A2006) with only
235 some very minor differences. Climate indices are calculated for each station and then
236 interpolated onto a regular grid, using a modified version of Shepard's angular distance
237 weighting (ADW) interpolation algorithm [*Shepard*, 1968]. The ADW gridding algorithm has
238 been used by a number of studies for gridding similar data sets of climate extremes [*Kiktev et*
239 *al.*, 2003; A2006], daily temperatures [*Caesar et al.*, 2006] or monthly climate variables [*New*
240 *et al.*, 2000] and has generally been shown to be a good method when gridding irregularly-
241 spaced data. Gridding the observations helps to solve several issues, including uneven station
242 distribution when calculating global averages [*Frich et al.*, 2002], and minimizing the impact
243 of data quality issues at individual stations due to averaging.

244

245 The ADW interpolation method requires knowledge of the spatial correlation structure of the
246 station data. We assume that station pairings greater than 2000km apart or stations with short
247 overlapping data will not provide meaningful correlation information. Therefore, correlations

248 between all station pairs within a 2000 km radius are calculated if there are overlapping data
249 for at least a 30-year period. Correlations are performed on all available data after 1951, the
250 period when most of the stations used in this study have good temporal coverage. However,
251 the correlation results are almost identical even if the period is extended back to 1901 (where
252 suitable station pairings are available). The inter-station correlations are then averaged into
253 100km bins and a second-order polynomial function is fitted to the resulting data assuming
254 that at zero distance the correlation function is equal to one. The decorrelation length scale
255 (DLS) is defined as the distance at which the correlation function falls below $1/\exp(1)$ and
256 represents the maximum ‘search radius’ in which station data are considered for the
257 calculation of grid point values. In addition the polynomial function is tested to determine
258 whether it is a good fit to the data at the 5% significance level using a chi-square statistic (for
259 an example of this type of function see Fig. A1 of Alexander et al. [2006]). If not, then the
260 decorrelation length scale is set to 200km, the minimum value set for search radius distance.
261 This differs slightly from HadEX where the minimum DLS was set to 100km, but it was
262 decided for HadEX2 that this minimum value should be more reflective of the size of the grid
263 boxes that were being used. However, for most indices and latitude bands DLS values above
264 200km are calculated, so this minimum DLS value will not be used in most cases. Only for
265 the annual Rx1day, R99p and CWD the minimum DLS is used at a number of latitudes with
266 land cover (e.g. Fig. 1d).

267
268 Decorrelation length scale values are calculated for each index separately. As in HadEX, DLS
269 values are calculated independently for four non-overlapping 30°-latitude zonal bands
270 between 90°N and 30°S, plus a 60° band spanning the data-sparse 30 to 90°S latitudes. For
271 indices with monthly output, the DLS is calculated for both the monthly and annual index
272 values. Linear interpolation is used to smooth the DLS values between bands in order to get a

273 separate value for each 2.5° latitude band. For comparison with HadEX, we chose the same
274 3.75° x 2.5° longitude-latitude grid. Examples of the DLS values are given in Figs. 1b,d.
275 The inter-station correlations, and thus the DLS, are, expectedly, generally larger for the
276 temperature-based indices than for the precipitation extremes and for monthly rather than
277 annual values.

278
279 Grid box values are calculated based on all station data within the DLS and weighted
280 according to their distance from the grid box center using a modified version of Shepard's
281 ADW interpolation algorithm (see equation A2 of Appendix A in A2006). A minimum of 3
282 stations is required to be within the DLS before a grid box value can be calculated; otherwise
283 a missing data value is assigned. The weight decays exponentially with increasing distance,
284 but additional information relating to the angle of the locations of the stations to each grid
285 box centre is also included to account for how bunched or isolated the stations are within the
286 search radius. An additional parameter adjusts the steepness of the decay [A2006; *Caesar et*
287 *al.*, 2006]. Again for consistency with HadEX, we set this parameter equal to 4, as this was
288 found to provide a reasonable compromise between reducing the root mean squared error
289 (RMSE) between gridded and station data and spatial smoothing. However, for global,
290 continental and even regional averages, the results are almost identical when using values
291 between 1 and 10 for this parameter.

292
293 Besides updating HadEX for the most recent years, we also extended the gridded product,
294 although with limited coverage, back to the first half of the 20th century, calculating grids
295 over the period 1901 to 2010. In the next section we present trends for two periods: 1951-
296 2010 and 1901-2010. Trends are calculated for each gridbox assuming that index values for
297 the grid box are available for at least 66% of the years (i.e., 40 years out of 1951-2010 and 73

298 years out of the 1901-2010 period), and that data are available through at least 2003. In order
299 to avoid the spurious influence of varying spatial coverage, global timeseries of area-
300 weighted averages are calculated using only gridboxes that have at least 90% of data during
301 the periods presented (i.e., 54 years out of 1951-2003 and 99 years out of the 1901-2010
302 period). Note that, owing to limited spatial coverage, the “global timeseries” are not
303 representative for the entire globe, and rather should be understood as “area-averages of all
304 sufficiently covered regions”. Particularly for the 110-year period 1901-2010, the 90%
305 completeness criterion restricts the grid boxes contributing to the “global timeseries” to grid
306 boxes from North America, Euroasia, Australia and parts of southern South America and
307 India (precipitation-only). Presented trends are calculated using Sen’s trend estimator [*Sen*,
308 1968] and trend significance is estimated at the 5 % level using the Mann-Kendall test
309 [*Kendall*, 1975]. This method was chosen because it makes no assumptions about the
310 distribution of the variable, and some of the climate indices do not follow a Gaussian
311 distribution. Note that a linear trend is not necessarily the best fit for the changes during the
312 periods presented. However, it is an easily understandable measure to document the changes
313 in the climate indices.

314

315 **4. Results**

316

317 Trends (shown as maps) are presented using data for each index for 110 years since 1901 and
318 for 60 years since 1951, when spatial coverage is more complete and other observational data
319 sets begin [e.g. *A2006*; *Caesar et al.*, 2006; *Donat et al.*, 2012a]. Hatching in Figures 3-9
320 indicates regions where trends are significant at the 5% level. Global average time series are
321 presented for the whole 1901-2010 period, and for comparison with HadEX also for 1951-
322 2003. Note that, owing to the 90% completeness criteria, the time series over the 1901-2010

323 period, mainly represent averages of grid boxes in North America, Eurasia, Australia, parts of
324 southern South America and India (precipitation-only).

Comentario [z2]: Repetition from newly inserted discussion 15lines above...either delete here, ore move above discussion down here...?

325
326 While trend maps can obviously highlight regional detail, the focus of this paper is to assess
327 broad scale changes in extremes. We therefore mostly limit our discussion of results to an
328 assessment of global change, acknowledging that regional studies can provide much more in-
329 depth analysis, although we do draw attention to interesting or unusual regional detail.

330

331 **4.1 Trends in annual temperature indices**

332

333 All temperature-related indices show significant and widespread warming trends, which are
334 generally stronger for indices calculated from daily minimum (night-time) temperature than
335 for those calculated from daily maximum (daytime) temperature.

336

337 For example, the frequency of cool nights based on daily minimum temperatures is shown to
338 have significantly decreased almost everywhere during the past 60 years (Fig. 3a). The
339 strongest reductions, up to 10 days per decade since 1951 (average annual frequency during
340 the 1961-1990 base period is by definition 36.5 days), are found over eastern Asia, northern
341 Africa and in some regions of South America. Globally averaged, cool night frequencies have
342 decreased by about 50 % (18 days in a year) from the 1950s to the first decade of the 21st
343 century. Correspondingly, at the upper tail of the minimum temperature distribution, we find
344 a significant increase in the frequency of warm nights in almost all regions (Fig. 3c). Globally
345 averaged the frequency of warm nights has increased by about 55 % (20 days in a year)
346 during the past 60 years. 97 % of the grid boxes with valid data show significant ($p \leq 0.05$)
347 increases in TN90p and decreases in TN10p, respectively (Table 3).

348

349 Analyzing day-time temperature extremes, we see a reduction in the number of cool days and
350 an increased frequency of warm days (Fig. 3b,d). The changes in cool and warm days appear
351 to be somewhat smaller compared to the cool and warm night frequency changes. The trends
352 are also spatially less homogeneous in sign, as slight cooling trends are found over eastern
353 North America (the so-called “warming hole”, *Portmann et al.*, 2009) and along the South-
354 American west coast areas (in particular the northern part of Chile). Still, in most regions and
355 in the global average there are significant warming trends towards less frequent cool and
356 more frequent warm days. In addition, 77 (84)% of the global land area covered by HadEX2
357 shows a significant increase in warm days (decrease in cool days) (see Table 3).

358

359 Mostly warming trends are also apparent when considering the absolute warmest and coldest
360 temperatures per year. The warming is generally stronger for the coldest than for the warmest
361 value. Since the middle of the 20th century, the coldest night (TNn) and coldest day (TXn) of
362 the year, for example, have significantly increased over much of Asia, North America,
363 Australia, and southern South America (Fig. 4a,b). Warming trends are particularly strong (up
364 to 1°C per decade) over large parts of Asia. 70 % (52 %) of the grid boxes with sufficient data
365 coverage show significant increases in TNn (TXn) during 1951 to 2010, whereas significant
366 decreases are only found in 3 % (4 %) of the grid boxes (Table 3). Globally averaged, the
367 temperature related to the coldest night of the year (TNn) has increased by about 3°C in the
368 past 60 years.

369

370 Warming (but mostly weaker) trends, are also found for temperatures related to the warmest
371 night (TNx) and the warmest day (TXx) over much of Europe, Asia and northeastern North
372 America, whereas a significant decrease in TXx is found over the eastern US and in South

373 America over parts of Argentina and Uruguay (Fig. 4c,d). On average globally, both TNx
374 and TXx have increased by about 1°C since the 1950s, however for TXx similarly high
375 values as today seem to have also occurred in the 1930s. Particularly high annual maximum
376 temperatures (TXx) occurred e.g. over North America in the 1930s. 64 % (32 %) of grid
377 boxes show significant increases in TNx (TXx), opposed by 3 % (6 %) with significant
378 decreases. Over most regions, the increases in TNn are stronger than increases in TXx.
379 Consequently the extreme temperature range (ETR) is reduced, in particular over North
380 America, Asia and South America, and also on global average (not shown).

381
382 Associated with the widespread warming trends, there is also a tendency towards shorter cold
383 spell duration (Fig. 5a) and, conversely, longer warm spell duration (Fig. 5b) in most areas.
384 These changes are significant for both indices over most of Eurasia. India stands out as
385 having much stronger increasing trends in WSDI than most other regions. Maximum
386 temperatures in India have increased by about 1.1°C since the beginning of the 20th century
387 with particularly large positive anomalies in the last couple of decades for both maximum and
388 minimum temperatures [IMD, 2012]. Owing to the stipulation of the 1961-1990 base period,
389 the region has experienced an excess of heatwave days since the mid-1990s by this definition
390 (also see e.g. Met Office, 2011) and this has inflated the trend in WSDI (see also discussion
391 section). On global average, the WSDI increased by approximately eight days since the
392 middle of the 20th century, however most of the increase happened in the most recent 30 years
393 after 1980. Conversely, the duration of cold spells has significantly decreased over large
394 areas, in global average by four days since 1950.

395
396 On centennial time scales, since the beginning of the 20th century, the warming trends show
397 mostly similar patterns to the trends since the middle of the last century. However, the trends

398 are more pronounced over the period 1951-2010 when compared to the period 1901-2010,
399 particularly for the frequency of warm/cold days/nights (Fig. 3). Also on the longer time scale
400 we find significant warming in the percentile-based indices over most parts of the world with
401 data coverage, except for daytime temperatures over the eastern US and southern South
402 America. Changes in the absolute values are less spatially coherent; however regions with
403 significant changes have the same sign of trend in both periods.

404

405 **4.2 Trends in seasonal temperature indices**

406

407 The warming trends related to the annual frequencies of warm/cool days/nights (Fig. 3) can
408 in general also be found throughout all seasons, however with differing magnitude and
409 significance. The seasonal results presented here were calculated as seasonal averages of the
410 monthly gridded fields. The frequency of warm days (Fig. 6), for example, shows a tendency
411 towards stronger and more extended warming during winter (i.e., DJF on northern
412 hemisphere and JJA on southern hemisphere) and the transition seasons than in summer,
413 particularly higher latitudes. For the two regions where local cooling trends were observed
414 (compare Fig. 3d), seasonal analysis shows that this cooling is most significant during the
415 summer months, i.e. June-August for the “warming hole” in North America and December-
416 February over South America, respectively.

417

418 The frequency of cool nights also decreases consistently throughout all seasons (Fig. 7).
419 Particularly over Asia this warming seems to be somewhat stronger during the cold months
420 than during summer. On the contrary, Europe and South America show stronger warming
421 during their respective summer months than in winter.

422

Comentario [z3]: Shall we include a sentence here that linear trend probably not most suitable measure...but understandable and comparable message?

423 **4.3 Trends in annual precipitation indices**

424

425 Although based on a larger number of stations (see Table 1), the gridded fields of the
426 precipitation indices exhibit generally a less widespread spatial coverage than the temperature
427 indices. This is because of the lower correlation of the precipitation measures between
428 neighboring stations (see Gridding method section and Fig. 1b,d).

429

430 The patterns of recent changes in precipitation indices appear spatially more heterogeneous
431 than the consistent warming pattern seen in the temperature indices. Most of the precipitation
432 indices show (partly significant) changes towards wetter conditions over the eastern half of
433 North America as well as over large parts of Eastern Europe, Asia and South America. Areas
434 with trends towards less extreme precipitation are observed e.g. around the Mediterranean, in
435 South-east Asia and the north-western part of North America. Such changes in extreme
436 precipitation are found, for example, for the number of heavy precipitation days (R10mm,
437 Fig. 8a) and the contribution from very wet days (R95pTOT, Fig. 8b). Globally averaged,
438 both indices display upward trends during the past 60 years. Similar patterns of change are
439 also found for the average intensity of daily precipitation (Fig. 8d). All precipitation-based
440 indices show larger areas with significant trends towards wetter conditions than areas with
441 drying trends (Table 3).

442

443 The number of consecutive dry days (CDD, Fig. 8c), a measure for extremely dry conditions,
444 also shows trends towards wetter conditions (i.e., fewer CDD) over larger parts of North
445 America, Europe and Southern Asia, whereas non-significant trends towards dryer conditions
446 are found over East Asia, eastern Australia, South Africa and portions of South America
447 where sufficient data are available for trend calculations. Globally no clear trend can be

448 identified.

449

450 As for the temperature indices, trends in the precipitation indices over the whole 1901-2010
451 period are largely similar in pattern to the trends since 1951 (where data are available),
452 however they are usually smaller in magnitude.

453

454 **4.4 Trends in seasonal precipitation indices**

455

456 Only two of the precipitation indices, Rx1day and Rx5day, have data available for sub-annual
457 timescales (see Table 1). We calculated the seasonal values of both indices as the seasonal
458 maxima of the monthly gridded fields. Their seasonal trends are generally comparable with
459 their annual trends (not shown). The annual maximum consecutive 5-day precipitations
460 amount, for example, displays significant tendencies towards stronger extreme precipitation
461 over eastern North America and large parts of Europe and Asia comparable with results
462 shown in Fig. 8. In these areas, the increase in extreme precipitation is visible across all
463 seasons (Fig. 9), but tends to be more significant during winter and autumn (DJF and SON in
464 Northern Hemisphere). Some tropical regions in South America and South-east Asia also
465 display a strong increase in extreme precipitation between 1951 and 2010 across the seasons,
466 particularly during December to May. However, as spatial coverage is limited for tropical
467 regions, a detailed investigation of this was not possible.

468

469 **5. Discussion**

470

471 Our results support previous studies, including A2006, that have found a shift in the
472 distribution of both maximum and minimum temperatures extremes consistent with warming,

473 and that globally averaged minimum temperature extremes are warming faster than
474 maximum temperature extremes. Recent studies have shown how the distributions of both
475 daily and seasonal temperatures have significantly shifted towards higher temperature values
476 since the middle of the 20th century [*Hansen et al., 2012; Donat and Alexander, 2012*],
477 including changes in higher statistical moments of the distributions and both would have
478 serious implications for climate impacts.

479
480 The driving mechanisms related to the reported changes may vary between regions and time
481 scales, but large scale natural variability plays a role [e.g. *Haylock et al., 2006; Barrucand et*
482 *al., 2008; Scaife et al., 2008; Alexander et al., 2009; Caesar et al., 2011; Renom et al.,*
483 *2011*], as do changes in anthropogenic greenhouse gases [e.g. *Kiktev et al., 2003; Alexander*
484 *and Arblaster, 2009; Min et al., 2011*] and land-use and land cover change [e.g. *Avila et al.,*
485 *2011*].

486
487 This study also indicates that on the whole the globally averaged trends in HadEX2
488 temperature and precipitation indices compare very well with the trends in HadEX over the
489 period when both datasets overlap and particularly when both datasets are masked with the
490 same gridboxes. Some minor differences in the time series of the global averages (mostly
491 towards the end of the series), for example TNx or CDD, largely vanish when the HadEX2
492 fields are masked to grid boxes where HadEX has non-missing data (dashed lines in Figs. 4
493 and 8). This shows that differences between area-averaged time series from both data sets can
494 mainly be explained by the different spatial coverage. Some larger differences during the last
495 years of comparison after 2000, as seen e.g. for TNn, TXn (Figs. 3a,b), R10mm or SDII (Figs
496 8a,d) can be explained by a drop of covered grid boxes in HadEX after 2000. The differences
497 would largely vanish if we applied an even stricter data completeness criterion, requiring e.g.

Comentario [z4]: May also include Pitman et al 2012..?

498 100% of data for grid cells to contribute to the global time series. The general similarity of
499 trends from both datasets, even given the largely different input data, gives additional
500 confidence in the robustness of the results.

501

502 There are two exceptions, however, in that there are some differences in the warm spell
503 (WSDI) and cold spell (CSDI) duration indices. For these two indices there are some larger
504 discrepancies between the new HadEX2 data set and HadEX and this is related to
505 inconsistencies in the calculation of these indices in HadEX. *Sillmann et al.*, [2012] discuss
506 how this is likely caused by the use of an earlier version of the RCLimDex/FClimDex code to
507 calculate indices for the USA which did not account for insufficient data precision (in part
508 due to rounding to whole degrees Fahrenheit) in the data, leading to a bias in the temperature
509 percentile exceedance rates estimated (this is discussed in *Zhang et al.*, 2009). Hence, caution
510 should be applied to analysis of CSDI and WSDI in HadEX especially over the North
511 American region, although other regions are fairly comparable. Owing to partly different
512 spell duration calculation between the two datasets, even masking HadEX2 to grid boxes
513 where HadEX had valid data (dashed blue line in Fig. 5) does not minimize the differences.
514 Indeed, the masked data are largely similar to the unmasked HadEX2 global WSDI and CSDI
515 averages. In the new HadEX2 dataset the indices were calculated using the same software for
516 all input stations, and the gridded fields do not suffer from such inconsistencies. However, by
517 definition these indices are statistically “volatile” in that they have a tendency to contain
518 many zeros and have no warm spells defined for periods shorter than 6 days, thus other heat
519 wave metrics that are more statistically robust are being proposed to replace them (Perkins
520 and Alexander, 2012). So that means even in HadEX2 some caution is required in assessing
521 results for the cold and warm spell duration indices.

522

Comentario [z5]: Not sure if this is needed, just wanted to make this explicit..?

523 While HadEX2 is a gridded dataset and therefore is likely to be used in future model
524 evaluation studies, we add a cautionary note that care must be taken to distinguish between
525 gridded products when evaluating extremes. In the method employed here, our output is more
526 closely representative of regularly spaced point locations. Climate model output and re-
527 analysis products more typically represent the area average of a grid. While in the case of a
528 lot of the temperature indices the two measures might be almost indistinguishable, for other
529 indices such as annual maxima or minima or those derived from daily precipitation, these
530 gridded metrics might represent quite different values [e.g. *Chen and Knutson, 2008*]. There
531 is some debate as to whether it would be more appropriate to grid the daily data first and then
532 calculate the indices as this might better reflect the measures that are returned by climate
533 models or reanalyses. However, calculating indices in this way would likely have the effect of
534 over-smoothing the extremes [*Hofstra et al., 2010*]. In addition it adds a level of structural
535 uncertainty into the resulting data, the effects of which have yet to be tested in detail [e.g.
536 *Donat et al., 2012a*]. However, interpolation of daily data was shown to reduce the intensity
537 of extremes [*Haylock et al., 2008*] and is argued to make them more comparable with climate
538 model data. We therefore recommend that these caveats are taken into account when using
539 HadEX2 for model evaluation.

540

541 **6. Conclusions**

542

543 We present a new global land-based gridded dataset of climate extremes indices. This dataset,
544 HadEX2, is the outcome of major data collection efforts and it substantially enhances a
545 previous dataset (HadEX, A2006) by providing improved spatial coverage, being updated for
546 the most recent years up to 2010, and extended back in time to the beginning of the 20th
547 century. The new dataset also solves some issues with regionally inconsistent calculations of

548 indices in HadEX. The analysis of recent changes in climate extremes largely confirms the
549 conclusions based on the previous dataset, hence generating increased confidence in the
550 robustness of the presented trends. The main findings include widespread and significant
551 warming trends related to temperature extremes indices, mostly stronger for indices based on
552 daily minimum temperatures than for indices calculated from daily maximum temperatures.
553 The changes in precipitation extremes are in general spatially more complex and mostly
554 locally less significant. However, on a global scale we find a tendency towards wetter
555 conditions for most precipitation indices.

556

557 It should be noted that there are still large data gaps over regions such as Africa and northern
558 South America, although international efforts are ongoing to try and fill in these gaps [e.g.
559 *Skansi et al.*, submitted to *Global and Planetary Change*] and to provide a data monitoring
560 capability for the ETCCDI indices [*Donat et al.*, 2012a]. At present though, the spatial
561 distribution of stations is still insufficient to provide a truly global picture of changes in
562 extremes, particularly for those extremes related to precipitation. It is hoped that efforts will
563 continue to address the need for continuous data collection and that ideally all data would be
564 shared with the international science community through a central data base (such as the
565 GHCN-Daily dataset). Note that all of the data presented in this paper, both station-based and
566 gridded indices, are available from www.climdex.org.

567

568 Acknowledgements

569

570 Donat, Alexander and Yang are supported by Australian Research Council grants
571 CE110001028 and LP100200690. Dunn, Willett and Caesar were supported by the Joint
572 DECC/Defra Met Office Hadley Centre Climate Programme (GA01101). Marengo, Renom

Comentario [z6]: Not sure if ALL station data will be available...? E.g. Arab-Region not?

573 and Rusticucci are supported by European Community's Seventh Framework Programme
574 (FP7/2007- 2013) Grant Agreement N° 212492: CLARIS LPB-A Europe- South America
575 Network for Climate Change Assessment and Impact Studies in La Plata Basin, Marengo also
576 from the FAPESP Assessment of Impacts and Vulnerability to Climate Change in Brazil and
577 strategies for Adaptation options project (Ref. 2008/581611) and Rusticucci also from
578 CONICET PIP-0227. National weather services from countries around the world are
579 acknowledged for providing observational data, explicit acknowledgement needs to be given
580 to the Sudan Meteorological Authority (SMA).

581

Comentario [z7]: Hope this does not sound too stupid this way..?

582 References

583 Aguilar, E., A.A. Barry, M. Brunet, L. Ekan, A. Fernandes, M. Massoukina, J. Mbah, A.
584 Mhanda, D.J. do Nascimento, T.C. Peterson, O.T. Uмба, M. Tomou, X. and Zhang, (2009),
585 Changes in temperature and precipitation extremes in western central Africa, Guinea
586 Conakry, and Zimbabwe, 1955-2006, *Journal of Geophysical Research-Atmospheres*, 114.

587
588 Alexander, L.V., X. Zhang, T.C. Peterson, J. Caesar, B. Gleason, A.M.G. Klein Tank, M.
589 Haylock, D. Collins, B. Trewin, F. Rahimzadeh, A. Tagipour, R Kumar Kolli, J.V. Revadekar,
590 G. Griffiths, L. Vincent, D.B. Stephenson, J. Burn, E. Aguilar, M. Brunet, M. Taylor, M.
591 New, P. Zhai, M. Rusticucci, J.L. Vazquez Aguirre, (2006), Global observed changes in daily
592 climate extremes of temperature and precipitation, *Journal of Geophysical Research-*
593 *Atmospheres* 111: D05109, doi:10.1029/2005JD006290

594
595 Alexander, L.V. and J.M. Arblaster, (2009), Assessing trends in observed and modelled
596 climate extremes over Australia in relation to future projections, *International Journal of*
597 *Climatology* 29: 417-435 DOI:10.1002/joc.1730

598
599 Alexander, L.V., P. Uotila, and N. Nicholls (2009), Influence of sea surface temperature
600 variability on global temperature and precipitation extremes, *Journal of Geophysical*
601 *Research-Atmospheres*, 114.

602
603 Avila, F.B., A.J., Pitman, M.G., Donat, L.V., Alexander, G., Abramowitz, (2012), Climate
604 model simulated changes in temperature extremes due to land cover change, *Journal of*
605 *Geophysical Research-Atmospheres*, 117, D04108, DOI: 10.1029/2011JD016382

606
607 Barrucand, M., M. Rusticucci, and W. Vargas, (2008), Temperature extremes in the south of
608 South America in relation to Atlantic Ocean surface temperature and Southern Hemisphere
609 circulation, *J. Geophys. Res.*, 113, D20111, doi:10.1029/2007JD009026

610
611
612
613 Caesar, J., L. Alexander, and R. Vose, (2006), Large-scale changes in observed daily
614 maximum and minimum temperatures: Creation and analysis of a new gridded data set,

615 *Journal of Geophysical Research-Atmospheres* 111: D05101, doi:10.1029/2005JD006280.
616

617 Caesar, J., L.V. Alexander, B. Trewin, K. Tse-ring, L. Sorany, V. Vuniyayawa, N. Keosavang,
618 A. Shimana, M.M. Htay, J. Karmacharya, D.A. Jayasinghearachchi, J. Sakkamart, E. Soares,
619 L.T. Hung, L.T. Thoung, C.T. Hue, N.T.T. Dung, P.V. Hung, H.D. Cuong, N.M. Cuong, S.
620 Sirabaha, (2011), Changes in temperature and precipitation extremes over the Indo-Pacific
621 region from 1971 to 2005, *International Journal of Climatology*, 31: 791-801. doi:
622 10.1002/joc.2118.
623

624 Chen, C.-T., and T. Knutson, (2008), On the verification and comparison of extreme rainfall
625 indices from climate models, *J. Climate*, 21(7), 1605–1621, doi:10.1175/2007JCLI1494.1.
626
627

628 Donat M.G., and L.V. Alexander, (2012), The shifting probability distribution of global
629 daytime and night-time temperatures, *Geophys. Res. Lett.*, doi:10.1029/2012GL052459, in
630 press.
631

632 Donat, M.G., I. Durre, H. Yang, L.V. Alexander, R. Vose, J. Caesar, (2012a), Global land-
633 based datasets for monitoring climatic extremes (submitted to *BAMS*)
634

635 Donat, MG., et al., (2012b), Changes of extreme temperature and precipitation in the Arab
636 region: long-term trends and variability related to ENSO and NAO (submitted to
637 *International Journal of Climatology*).
638

639 Durre, I., M. J. Menne, B. E. Gleason, T. G. Houston, and R. S. Vose, (2010), Comprehensive
640 automated quality assurance of daily surface observations, *Journal of Applied Meteorology*
641 *and Climatology*, 8, 1615-1633.
642
643

644 Frich, P., L.V. Alexander, P. Della-Marta, B. Gleason, M. Haylock, A. Klein Tank, T.
645 Peterson, (2002), Observed coherent changes in climatic extremes during the second half of
646 the 20th century, *Climate Research* 19: 193-212.
647

648 Hansen, J., M. Sato, and R. Ruedy, 2012: Perception of climate change. *Proc. Natl. Acad.*

649 *Sci.*, 109, 14726-14727, E2415-E2423, doi:10.1073/pnas.1205276109.

650

651 Haylock, M.R., Peterson, T.C., Alves, L.M., Ambrizzi, T., Anunciação, Y.M.T., Baez, J.,
652 Barros, V.R., Berlato, M.A., Bidegain, M., Coronel, G., Corradi, V., Garcia, V.J., Grimm,
653 A.M., Karoly, D., Marengo, J.A., Marino, M.B., Moncunill, D.F., Nechet, D., Quintana, J.,
654 Rebello, E., Rusticucci, M., Santos J.L., Trebejo, I., Vincent, L.A., (2006), Trends in total and
655 extreme South American rainfall 1960-2000 and links with sea surface temperature, *J. of*
656 *Climate*, 19, 1490-1512.

657

658 Haylock, M. R., N. Hofstra, A. M. G. Klein Tank, E. J. Klok, P. D. Jones, and M. New
659 (2008), A European daily high-resolution gridded data set of surface temperature and
660 precipitation for 1950–2006, *J. Geophys. Res.*, 113, D20119, doi:10.1029/2008JD010201.

661

662 Hofstra, N., M. New, and C. McSweeney (2010), The influence of interpolation and station
663 network density on the distributions and trends of climate variables in gridded daily data,
664 *Clim. Dynam.*, 35(5), 841–858, doi:10.1007/s00382-009-0698-1.

665

666 **India Meteorological Department (IMD), (2011), Annual climate summary.**

Comentario [z8]: Complete Reference?

667

668 Kendall, M.G. (1975) *Rank correlation methods*. Charles Griffin, London.

669

670 Kiktev, D., D. Sexton, L. Alexander, C. Folland (2003), Comparison of modelled and
671 observed trends in indicators of daily climate extremes, *Journal of Climate* 16(22): 3560-71.

672

673 Klok, E.J. and A.M.G. Klein Tank, (2009), Updated and extended European dataset of daily
674 climate observations, *International Journal of Climatology*, 29 (8), 1182-1191 DOI:
675 10.1002/joc.1779

676

677 Kruger, A.C., and S.S. Sekele, (2012), Trends in extreme temperature indices in South Africa:
678 1962–2009, *International Journal of Climatology*. DOI: 10.1002/joc.3455

679

680 Griffiths, G.M., M.J. Salinger, and I. Leleu (2003), Trends in extreme daily rainfall across the
681 South Pacific and relationships to the SPCZ, *International Journal of Climatology*, 23, 847-
682 869.

683
684
685 Mekis, É. and L.A. Vincent, (2011) An overview of the second generation adjusted daily
686 precipitation dataset for trend analysis in Canada, *Atmosphere-Ocean*, 49(2), 163-177.
687
688 Menne, M. J., I. Durre, B. G. Gleason, T. G. Houston, and R. S. Vose, (2012), An overview of
689 the Global Historical Climatology Network-Daily database, *Journal of Atmospheric and*
690 *Oceanic Technology*, 29, 897-910
691
692 Menne, M. J., and C. N. Williams Jr. (2005), Detection of undocumented changepoints using
693 multiple test statistics and composite reference series, *J. Clim.*, 18, 4271– 4286,
694 doi:10.1175/JCLI3524.1.
695
696 Met Office, (2011), Climate: observations, projections and impacts, published by Met Office,
697 available at [http://www.metoffice.gov.uk/climate-change/policy-relevant/obs-projections-](http://www.metoffice.gov.uk/climate-change/policy-relevant/obs-projections-impacts)
698 [impacts](http://www.metoffice.gov.uk/climate-change/policy-relevant/obs-projections-impacts).
699
700 Min, S.-K., X. Zhang, F. W. Zwiers, and G. C. Hegerl, (2011), Human contribution to more-
701 intense precipitation extremes, *Nature*, 470(7334), 378–381, doi:10.1038/nature09763.
702
703
704 Morak, S., G. Hegerl G, J. Kenyon, (2011), Detectable Regional Changes in the Number of
705 Warm Nights. *Geophys Res Lett*, doi:10.1029/2011GL048531.
706
707 New, M. G., M. Hulme, and P. D. Jones, (2000), Representing twentieth century space-time
708 climate variability. Part II: Development of 1901–96 monthly grids of terrestrial surface
709 climate, *J. Clim.*, 13, 2217–2238.
710
711 Nicholls, N. and L. Alexander, (2007), Has the climate become more variable or extreme?
712 Progress 1992–2006. *Prog Phys Geog* 2007. 31:1–11.
713
714 Oria, C., (2012), Tendencia actual de los indicadores extremos de cambio climático en la
715 cuenca del rio Mantaro, Technical Note of the Centro de Predicción Numérica/Dirección
716 General de Meteorología Servicio Nacional de Meteorología e Hidrología, Perú.

Comentario [z9]: Check reference...can this be completed?

717
718 Perkins, S.E., and L.V. Alexander, (2012), On the measurement of heatwaves, *Journal of*
719 *Climate* (submitted 21st June 2012).
720
721 Peterson, T.C., and M. J. Manton, (2008), Monitoring changes in climate extremes: a tale of
722 international collaboration, *Bulletin of the American Meteorological Society*, 89, 1266–1271.
723 DOI:10.1175/2008BAMS2501.1
724
725 Peterson, T. C., X. B. Zhang, M. Brunet-India, and J. L. Vazquez-Aguirre, (2008), Changes in
726 North American extremes derived from daily weather data, *J. Geophys. Res.-Atmos.*,
727 113(D7), D07113
728
729 Portmann, R.W., S. Solomon, and G. C. Hegerl, (2009), Spatial and seasonal patterns in
730 climate change, temperatures, and precipitation across the United States, *Proc. Nat. Acad.*
731 *Sci.*, 106, 7324-7329, doi:10.1073/pnas.0808533106.
732
733
734 Renom M., M. Rusticucci, and M. Barreiro, (2011), Multidecadal changes in the relationship
735 between extreme temperature events in Uruguay and the general atmospheric circulation.
736 *Climate Dynamics*, 37 (11-12), pp. 2471-2480
737
738 Rusticucci, M., (2012), Observed and simulated variability of extreme temperature events
739 over South America, *Atmospheric Research* 106 (2012) 1–17
740
741 Rusticucci, M., J. Marengo, O. Penalba, M. Renom, (2010), An intercomparison of model-
742 simulated extreme rainfall and temperature events during the last half of twentieth century.
743 Part 1 : Mean values and variability, *Climatic Change*, Volume 98, Issue 3, 493-508
744
745 Rusticucci, M. and M., Renom, (2008), Variability and trends in indices of quality-controlled
746 daily temperature extremes in Uruguay, *International Journal of Climatology*, 28:1083-1095,
747 DOI: 10.1002/joc.1607.
748
749 Salinger, M.J., and G. Griffiths, (2001), Trends in annual New Zealand daily temperature and
750 rainfall extremes, *International Journal of Climatology*, 21, 1437-1452.

751
752 Scaife, A. A., C. K. Folland, L. V. Alexander, A. Moberg, and J. R. Knight, (2008), European
753 climate extremes and the North Atlantic Oscillation, *Journal of Climate*, 21, 72-83.
754
755 Sen, P. K., (1968), Estimates of the regression coefficient based on Kendall's Tau, *J. Am. Stat.*
756 *Assoc.*, 63, 1379– 1389.
757
758 Shepard, D., (1968), A two-dimensional interpolation function for irregularly spaced data,
759 paper presented at 23rd National Conference, *Assoc. for Comput. Mach.*, New York.
760
761 Sillmann, J., and E., Roekner, (2008), Indices for extreme events in projections of
762 anthropogenic climate change, *Climatic Change*, 86(1–2), 83–104.
763
764 Sillmann et al., 2012. Climate extreme indices in the CMIP5 multi-model 1 ensemble. Part 1:
765 Model evaluation in the present climate. *J. Geophys. Res.* (submitted)
766
767
768
769
770 Trewin, B., (2012), A daily homogenized temperature data set for Australia. *International*
771 *Journal of Climatology*, (online first), DOI: 10.1002/joc.3530
772
773 Villarroel, C., B. Rosenblüth and P. Aceituno 2006. Climate change along the extratropical
774 west coast of South America (Chile): Daily max/min temperatures. 8 ICSHMO, Foz de
775 Iguazu, April 2006
776
777 Vincent, L.A., E. Aguilar, M. Saindou, A.F. Hassane, G. Jumaux, D. Roy, P. Booneedy, R.
778 Virasami, L.Y.A. Randriamarolaza, F.R. Faniriantsoa, V. Amelie, H. Seeward, and B.
779 Montfraix, (2011), Observed trends in indices of daily and extreme temperature and
780 precipitation for the countries of the western Indian Ocean, 1961-2008, *J. Geophys. Res.*, 116,
781 D10108, doi:10.1029/2010JD015303.
782
783 Vincent, L. A., X. L. Wang, E. J. Milewska, H. Wan, F. Yang, and V. Swail (2012). A second
784 generation of homogenized Canadian monthly surface air temperature for climate trend

Comentario [z10]: Reference not clear
– is this a conference proceeding?

785 analysis, *J. Geophys. Res.*, 117, D18110, doi:10.1029/2012JD017859.
786
787
788 Zhai, P. M., and P. Xiaohua, (2003), Trends in temperature extremes during 1951-1999 in
789 China, *Geophys. Res. Lett.*, 30 (17): 1913, doi:10.1029
790
791 Zhai, P., X. Zhang, H. Wan, and X. Pan (2005), Trends in total precipitation and frequency of
792 daily precipitation extremes over China, *J. Clim.*, 18, 1096–1108
793
794 Zhang, X., L. Alexander, G.C. Hegerl, P. Jones, A. Klein Tank, T.C. Peterson, B. Trewin, and
795 F.W. Zwiers, (2011), Indices for monitoring changes in extremes based on daily temperature
796 and precipitation data, *WIREs Climate Change*, 2:851–870. doi:10.1002/wcc.147.
797
798 Zhang, X., G. Hegerl, F. Zwiers, and J. Kenyon, (2005), Avoiding inhomogeneity in
799 percentile-based indices of temperature extremes, *J. Clim.*, 18, 1641– 1651.
800
801 Zhang, X., F.W. Zwiers, G. Hegerl, (2009), The influence of data precision on the calculation
802 of temperature percentile indices, *Int J Climatol*, 29: 321–327. DOI:10.1002/joc.1738.
803
804 Zwiers, F.W., L.V. Alexander, G.C. Hegerl, J.P. Kossin, T.R. Knutson, P. Naveau, N.
805 Nicholls, C. Schär, S.I. Seneviratne, X. Zhang, M. Donat, O. Krueger, S. Morak, T.Q.
806 Murdock, M. Schnorbus, V. Ryabin, C. Tebaldi, X.L. Wang, (2012). Challenges in Estimating
807 and Understanding Recent Changes in the Frequency and Intensity of Extreme Climate and
808 Weather Events. In: *Climate Science for Serving Society: Research, Modelling and Prediction*
809 *Priorities*. G. R. Asrar and J. W. Hurrell, Eds. Springer, in press.
810

811 Figure Captions

812

813 **Fig. 1:** Maps indicate locations of stations used in HadEX2 for an example temperature index
814 (a) TXx and precipitation index (c) Rx1day. Sources of data (see text) are color-coded. The
815 right panel (b) and (d) shows the decorrelation length scales (in km) for each latitude band for
816 TXx and Rx1day respectively for Annual (solid line), January (dotted line) and July (dashed
817 line). Thin grey lines indicate the borders of latitude bands used for grouping the stations
818 when calculating the decorrelation length scales (see text for details).

819

820 **Fig. 2:** Time series of annual grid box coverage (out of a total of 2382 land grids for the
821 chosen longitude-latitude grid) for (a) TXx and (b) Rx1day from 1901 to 2010 for HadEX2
822 and 1951 to 2003 for HadEX (A2006) after the gridding algorithm has completed (see text
823 for details). Top panel shows the total number of grid boxes with non-missing data globally,
824 bottom panel shows the percentage of land grid boxes with non-missing data for each
825 latitude.

826

827 **Fig. 3:** Trends (in annual days per decade, shown as maps) for annual series of percentile
828 temperature indices for (left) 1901-2010 and (middle) 1951-2010 for cool nights (TN10p),
829 warm nights (TN90p), cool days (TX10p), and warm days (TX90p). Trends were calculated
830 only for grid boxes with sufficient data (at least 66 % of years having data during the period
831 and the last year of the series is no earlier than 2003). Hatching indicates regions where
832 trends are significant at the 5% level. The time series show the global average annual
833 anomalies (in days per year) for the same indices relative to 1961–1990 mean values for
834 HadEX2 (blue lines) over the 1901-2010 period, and a comparison with HadEX (red line;
835 A2006) over the 1951-2003 period (for which HadEX provided data) is also shown. The

836 thick blue line shows the 21-point Gaussian filtered data for HadEX2. Note that for the global
837 average time series only grid boxes with at least 90% of temporal coverage are used, i.e. 99
838 years during 1901-2010 and 48 years during 1951-2003 (see text).

839

840 **Fig. 4:** As Figure 3 but for annual series of indices (a) coldest night (TNn) in °C, (b) coldest
841 day (TXn) in °C, (c) warmest night (TNx) in °C, and (d) hottest day (TXx) in °C. The time
842 series show annual anomalies (in °C) as described in Figure 3. In the comparison with
843 HadEX (1951-2003), the HadEX2 time series masked to HadEX grid boxes is also shown
844 (dashed blue line).

845

846 **Fig. 5:** Trends (in annual days per decade) for the period 1951– 2010 for cold spell duration
847 index (CSDI) and warm spell duration index (WSDI) in HadEX2. Missing data and
848 significance criteria as in Figure 3. Timeseries plots compare HadEX and HadEX2 global
849 averages and highlight issues with the calculation of these indices in HadEX (see text).

850

851 **Fig. 6:** Trends (in days per decade) for seasonal series of warm days (TX90p) for the period
852 1951– 2010 for (a) December-February, (b) June-August, (c) March-May, and (d) September-
853 November. Trends were calculated using same criteria as in Fig. 3.

854

855 **Fig. 7:** As Figure 6 but for cool nights (TN10p).

856

857 **Fig. 8:** As Figure 3 but for decadal trends in annual series of indices (a) Number of heavy
858 precipitation days (R10) in days, (b) contribution from very wet days (R95pTOT) in %, (c)
859 consecutive dry days (CDD) in days and (d) simple daily intensity index (SDII) in mm/day.
860 The time series show annual anomalies as described in Figure 3. In the comparison with

861 HadEX (1951-2003), the HadEX2 time series masked to HadEX grid boxes is also shown
862 (dashed blue line).

863

864 **Fig. 9:** As Figure 6 but for seasonal trends (in mm/decade) in maximum 5-day precipitation
865 (Rx5day).

866

867

868

869 Tables

870 **Table 1:** The extreme temperature and precipitation indices available in HadEX2 along with
 871 the number of stations that was included for each index. Most indices are recommended by
 872 the ETCCDI (see http://cccma.seos.uvic.ca/ETCCDI/list_27_indices.html) except those
 873 marked with an asterisk. Indices in bold represent those that are also available monthly.

ID	Indicator name	Indicator definitions	Units	Number of stations
TXx	Max Tmax	Monthly maximum value of daily max temperature	°C	7381
TNx	Max Tmin	Monthly maximum value of daily min temperature	°C	7390
TXn	Min Tmax	Monthly minimum value of daily max temperature	°C	7381
TNn	<u>Min Tmin</u>	Monthly minimum value of daily min temperature	°C	73
TN10p	Cool nights	Percentage of time when daily min temperature < 10 th percentile	%	66
TX10p	Cool days	Percentage of time when daily max temperature < 10 th percentile	%	6623
TN90p	Warm nights	Percentage of time when daily min temperature > 90 th percentile	%	6621
TX90p	Warm days	Percentage of time when daily max temperature > 90 th percentile	%	6602
DTR	Diurnal temperature range	Monthly mean difference between daily max and min temperature	°C	7365
GSL	Growing season length	Annual (1st Jan to 31st Dec in NH, 1st July to 30th June in SH) count between first span of at least 6 days with TG>5°C and first span after July 1 (January 1 in SH) of 6 days with TG<5°C (where TG is daily mean temperature)	Days	6843
ID	Ice days	Annual count when daily maximum temperature < 0°C	Days	7120
FD	Frost days	Annual count when daily minimum temperature < 0°C	Days	7150
SU	Summer days	Annual count when daily max temperature > 25°C	Days	7168
TR	Tropical nights	Annual count when daily min temperature > 20°C	Days	7179
WSDI	Warm spell duration indicator	Annual count when at least 6 consecutive days of max temperature > 90 th percentile	Days	6600
CSDI	Cold spell duration indicator	Annual count when at least 6 consecutive days of min temperature < 10 th percentile	Days	6594
RX1day	Max 1-day precipitation amount	Monthly maximum 1-day precipitation	Mm	11588
RX5day	Max 5-day precipitation amount	Monthly maximum consecutive 5-day precipitation	Mm	11607
SDII	Simple daily intensity index	The ratio of annual total precipitation to the number of wet days (≥ 1 mm)	mm/day	11607
R10mm	Number of heavy precipitation days	Annual count when precipitation ≥ 10 mm	Days	11607
R20mm	Number of very heavy precipitation days	Annual count when precipitation ≥ 20 mm	Days	11588
CDD	Consecutive dry days	Maximum number of consecutive days when precipitation < 1 mm	Days	11602
CWD	Consecutive wet days	Maximum number of consecutive days when precipitation ≥ 1 mm	Days	11583
R95p	Very wet days	Annual total precipitation from days > 95 th percentile	Mm	11588
R99p	Extremely wet days	Annual total precipitation from days > 99 th percentile	Mm	11588

Comentario [z11]: Shall we call these indices coldest night, warmest night, coldest day, hottest day?

PRCPTOT	Annual total wet-day precipitation	Annual total precipitation from days ≥ 1 mm	Mm	11588
*ETR	Extreme temperature range	TXx – TNn	°C	7159
*R95pTOT	Contribution from very wet days	$100 * R95p / PRCPTOT$	%	11308
*R99pTOT	Contribution from extremely wet days	$100 * R99p / PRCPTOT$	%	11308

874

875 **Table 2:** References and contacts for data used to create HadEX2. In most cases the indices
876 were calculated by the contact author and sent to the lead author for inclusion in HadEX2.

Source region/Dataset	Contact	Reference(s) if available
Arab region workshop	Paper author: m.donat@unsw.edu.au	<i>Donat et al. [2012b]</i>
Argentina	Paper author: mati@at.fcen.uba.ar	<i>Rusticucci, [2012]</i>
Australia	Paper author: b.trewin@bom.gov.au	<i>Trewin, [2012]</i>
Brazil	http://www.inmet.gov.br , jose.marengo@inpe.br	
Canada	Paper authors: Lucie.Vincent@ec.gc.ca (for temperature); Eva.Mekis@ec.gc.ca (for precipitation)	<i>Mekis and Vincent, [2011]; Vincent et al., [2012]</i>
Chile	Paper author: cvilla@meteochile.com	<i>Villarroel et al., [2006]</i>
China	Chinese Meteorological Administration (CMA)	<i>Zhai et al., [2005]; Zhai et al., [2003]</i>
Congo workshop	Paper authors: enric.aguilar@urv.cat ; Xuebin.zhang@ec.gc.ca ; manola.brunet@urv.cat	<i>Aguilar et al., [2009]</i>
ECAD	The European Climate Assessment and Dataset: http://eca.knmi.nl/	<i>Klok and Klein Tank, [2009]</i>
HadEX	Climdex project: http://www.climdex.org	<i>Alexander et al., [2006]</i>
India	Paper author: aks_ncc2004@yahoo.co.in	
Latin America	Latin American Climate Assessment and Dataset: http://lacad.ciifen-int.org/download/millennium/millennium.php	
New Zealand	Paper author: salinger@stanford.edu	<i>Griffiths et al., [2003], Salinger and Griffiths, [2001]</i>
Peru	Paper author: clara@senamhi.gob.pe	<i>Oria, [2012]</i>
South Africa	Paper authors: hewitson@csag.uct.ac.za ; Andries.Kruger@weathersa.co.za ; cjack@csag.uct.ac.za	<i>Kruger and Sekele, [2012]</i>
South-east Asia	Southeast Asian Climate Assessment and Dataset: http://saca-bmkg.knmi.nl/	
Uruguay	Paper author: renom@fisica.edu.uy	<i>Rusticucci and Renom, [2008]</i>
USA	Global Historical Climatology Network – Daily: http://www.ncdc.noaa.gov/oa/climate/gHCN-daily/	<i>Durre et al., [2010]; Menne et al., [2012]; Peterson et al., [2008]</i>
Vietnam workshop	Paper author: john.caesar@metoffice.gov.uk	<i>Caesar et al., [2011]</i>
West Indian Ocean workshop	Paper author: Lucie.Vincent@ec.gc.ca	<i>Vincent et al., [2011]</i>

877
878

879 **Table 3:** Land-based grid boxes filled by data meeting the data completeness criteria (see
880 text) for each index along with the percentage of those gridboxes that show either a
881 significant increase or decrease at the 5% level during the 1951-2010 period.

Index	Number of land-based grid boxes	% significant increase	% significant decrease
TXx	1110	32.16	5.95
TNx	1056	63.73	3.22
TXn	1333	52.21	4.05
TNn	1336	70.36	3.14
TN10p	1398	0.36	96.92
TX10p	1400	0.36	84
TN90p	1316	97.49	0
TX90p	1437	76.55	1.25
DTR	1079	8.9	59.31
GSL	948	54.01	2.22
ID	1186	1.85	49.75
FD	1278	3.05	67.37
SU	1271	46.66	6.61
TR	1032	48.74	4.36
WSDI	1182	69.63	0.59
CSDI	1005	3.18	68.96
RX1day	420	21.9	7.14
RX5day	438	23.97	8.22
SDII	880	46.48	8.64
R10	853	28.96	10.32
R20	568	28.87	9.15
CDD	832	5.77	21.15
CWD	435	18.39	11.03
R95p	561	30.66	5.88
R99p	420	25	4.05
PRCPTOT	1022	40.8	10.18
ETR	1207	5.3	50.7
R95pTOT	546	23.08	5.13
R99pTOT	409	20.05	3.91

882